

# Structural bases of electron transfer and reaction cycle of ring-hydroxylating dioxygenase systems

Hideaki NOJIRI

Biotechnology Research Center, The University of Tokyo

**Report:** Using carbazole (CAR) 1,9a-dioxygenase (CARDO), crystal structures of reduced ferredoxin component ( $Fd_{red}$ ), CAR-bound reduced oxygenase component ( $Oxy_{red/red}$ ; see Fig. 1), both CAR- and  $O_2$ -bound oxidized Oxy ( $Oxy_{ox/ox}$ ), and product-bound  $Oxy_{ox/ox}$  were solved. These are found in the catalytic cycle of CARDO and clearly show the molecular action of the enzyme from the reduction of Oxy by  $Fd_{red}$  to product formation. In addition, mutant analyses show that the Fd-binding site of  $\alpha_3\beta_3$ -type Oxy is located on the side of Oxy mushroom structure, distinct from that in  $\alpha_3$ -type CARDO Oxy.

## Research aims

Our previous studies clarified the crystal structures of oxidized Oxy ( $Oxy_{ox/red}$ , I in Fig. 1)<sup>1)</sup>, oxidized Fd ( $Fd_{ox}$ , II)<sup>2)</sup>, and the complex of  $Oxy_{ox/red}:Fd_{ox}$  (III)<sup>4)</sup>. Although these structures provided basic information on the structures and functions of CARDO, structural bases of Oxy reduction and product formation were still limited. In this study, we solved the crystal structures of reduced Fd ( $Fd_{red}$ , IV) and the substrate-, oxygen-, and product-binding structures (VII, VIII, IX). Together with the structures of the complex of  $Oxy_{red/red}:Fd_{ox}$  and  $Oxy_{red/red}$  (Matsuzawa *et al.*, in preparation), we clarified the molecular mechanism of  $Oxy_{ox/red}$  reduction and product formation. On the other hand, we accessed whether the Fd-binding site of  $\alpha_3\beta_3$ -type Oxy is the same as that in  $\alpha_3$ -type CARDO Oxy.

## Methods

$Fd_{red}$  was crystalized under anaerobic conditions, and its crystal structure was solved. Using the V crystals soaked with CAR, or both CAR and  $O_2$ , the crystal structures of VII, VIII, and IX were solved. As the  $\alpha_3\beta_3$ -type Oxy, it was used in a cumene 2,3-dioxygenase (CDO) system. Ala replacements were introduced into putative binding sites between Oxy and Fd in the CDO system, and Oxy-reduction activity in the reconstituted CDO system was assessed.

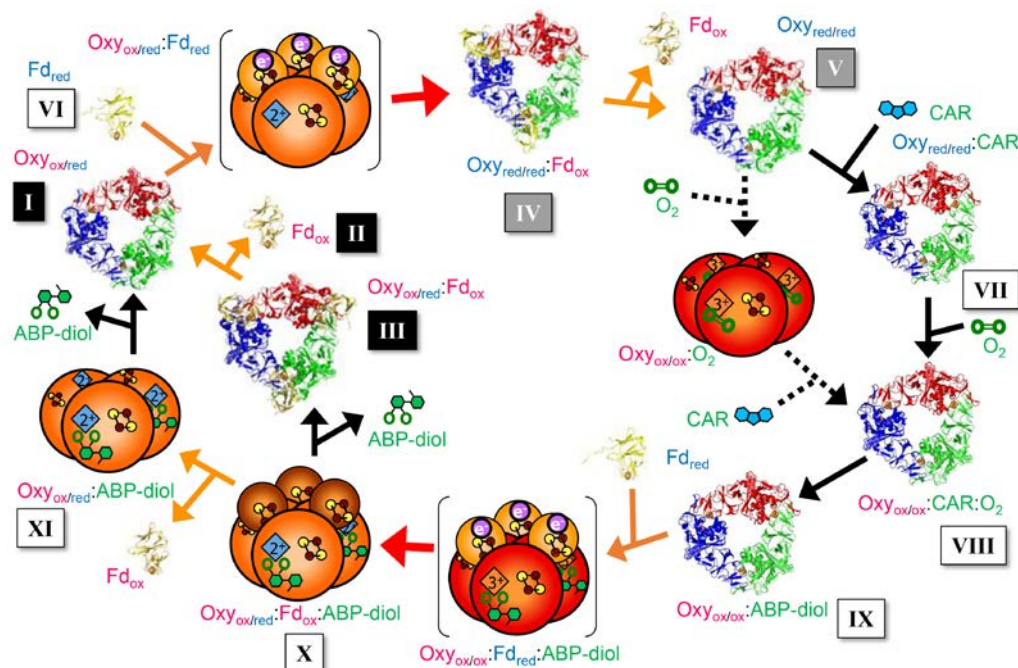


Fig. 1. Catalytic cycle of CARDO Oxy

Lowercase “ox” and “red” indicate the “oxidized” and “reduced” states, respectively, of Oxy ([2Fe:2S] cluster/active site iron) and Fd ([2Fe:2S] cluster).

## Results

The crystal structure of Fd<sub>red</sub> (VI) was solved at 1.8 Å resolution. Because rapid electron transfer could occur after Fd<sub>red</sub>-binding to I, it could be difficult to solve the crystal structure of the state shown in parentheses in Fig. 1. Therefore, we instead used the Oxy structure of III, because the redox states of Oxy in both crystals are the same, and the structural changes from I to V were analyzed. Among the structural changes, the movement of Oxy Arg118 side chain was important (Fig. 2A). The side chain of Arg118 constituted salt bridges with Fd Glu43 upon Fd binding (Fig. 2A Left). After electron transfer, the salt bridge broke and the Arg118 side chain formed a hydrogen bond with the Oxy amino acid residue (Fig. 2A Center and Right). Similar movement was observed in Oxy Arg210, and these two are considered to be an important switch for Fd association/dissociation. The CAR-binding structure of Oxy<sub>red/red</sub> (VII) and its O<sub>2</sub>-exposed structure was also solved (both at 2.2 Å resolution). In the latter structure, both CAR and O<sub>2</sub> were bound at one active site (VIII), while the products were bound at other two sites (IX). In the product-bound structure (IX), two phenyl moieties are twisted (Fig. 2B). As shown in Fig. 2C, a water molecule bound at the active site iron was removed upon CAR-binding, and O<sub>2</sub> bound at the resultant vacant position (Fig. 2C).

Two possible Fd-binding sites were predicted for the α<sub>3</sub>β<sub>3</sub>-type Oxy-specific mushroom structure; the upper part corresponds to that in CARDO Oxy (α subunit) and the

side part is constituted by both  $\alpha$  and  $\beta$  subunits. We introduced Ala to Asp158, Trp159, Glu180, and Arg407 of  $\alpha$  subunit (upper); Lys117 and Lys141 of  $\alpha$  subunit; and Arg65, Leu98, and Trp100 of  $\beta$  subunit (side). As a result, the Oxy-reducing activities were reduced in Lys117Ala (to less than 20%) and Arg65Ala (to 40~60%), suggesting that Fd could bind at the side part of the  $\alpha_3\beta_3$ -type mushroom-like Oxy.

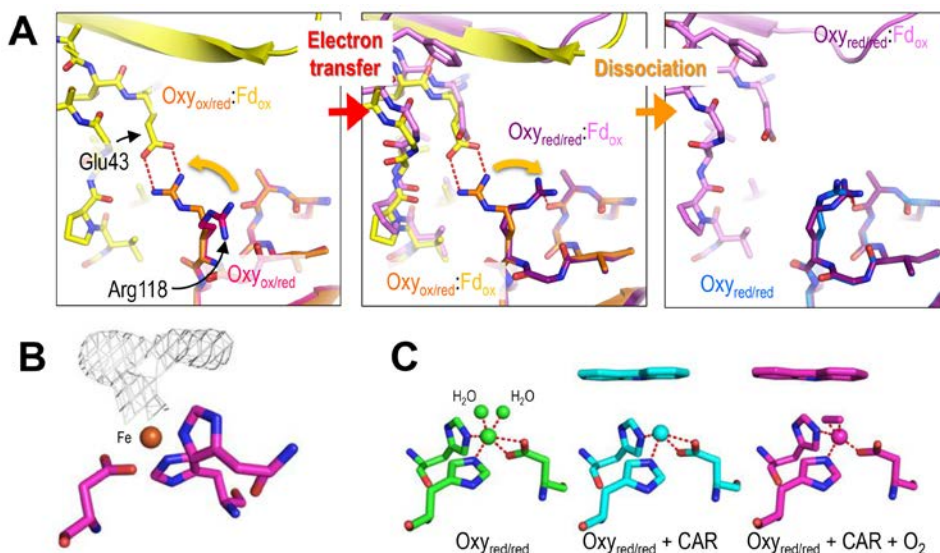


Fig. 2. Structure comparisons reveal the structural changes specific for Fd association/dissociation (A) and CAR-binding followed by product formation (B, C)

## Conclusion

We succeeded in clarifying the crystal structures of VI, VII, VIII, and IX in the catalytic cycle of CARDO Oxy (Fig. 1). The next targets are X and XI, which would allow us to clarify a complete picture of the catalytic cycle. Based on the results on the putative Fd-binding state of  $\alpha_3\beta_3$ -type Oxy, we plan to evaluate the binding affinities of amino acid-replaced enzymes and to determine the complex structure of  $\alpha_3\beta_3$ -type Oxy and Fd.

## References

- 1) Nojiri, H. *et al.*, (2005) Structure of the terminal oxygenase component of angular dioxygenase, carbazole 1,9a-dioxygenase. *J. Mol. Biol.* **351**:355-370.
- 2) Nam, J.-W. *et al.*, (2005) Crystal structure of the ferredoxin component of carbazole 1,9a-dioxygenase of *Pseudomonas resinovorans* strain CA10, a novel Rieske non-heme iron oxygenase system. *Proteins* **58**:779-789.
- 3) Ashikawa *et al.*, (2006) Electron transfer complex formation between oxygenase and ferredoxin components in Rieske nonheme iron oxygenase system. *Structure* **14**:1779-1789.
- 4) Dong, X. *et al.* (2005) Crystal structure of the terminal oxygenase component of cumene

dioxygenase from *Pseudomonas fluorescence* IP01. *J. Bacteriol.* **187**:2483-2490.